AD-A057 478 AIR FORCE GEOPHYSICS LAB HANSCOM AFB MASS F/G 4/1
AIRGLOW CALCULATIONS FOR REMOTE SENSING OF DENSITY.(U)
MAY 78 R A VAN TASSEL
UNCLASSIFIED AFGL-TR-78-0115 NL

1 OF 1
AD
A057 478

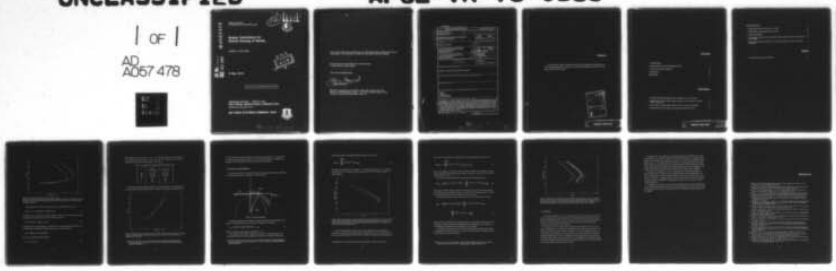

END
DATE
FILMED
9-78
DDC

AFGL-TR-78-0115
AIR FORCE SURVEYS IN GEOPHYSICS, NO. 386

12 LEVEL

Airglow Calculations for Remote Sensing of Density

ROGER A. VAN TASSEL

5 May 1978

AERONOMY DIVISION PROJECT 6688
AIR FORCE GEOPHYSICS LABORATORY
HANSCOM AFB, MASSACHUSETTS 01731

AIR FORCE SYSTEMS COMMAND, USAF

This report has been reviewed by the ESD Information Office (OI) and is releasable to the National Technical Information Service (NTIS).

This technical report has been reviewed and is approved for publication.

FOR THE COMMANDER

John Howard

Chief Scientist

Qualified requestors may obtain additional copies from the Defense Documentation Center. All others should apply to the National Technical Information Service.

Unclassified

SECURITY CLASSIFICATION OF THIS PAGE *(When Data Entered)*

REPORT DOCUMENTATION PAGE

READ INSTRUCTIONS BEFORE COMPLETING FORM

1. REPORT NUMBER: AFGL-TR-78-0115	2. GOVT ACCESSION NO.
3. RECIPIENT'S CATALOG NUMBER	
4. TITLE *(and Subtitle)*: AIRGLOW CALCULATIONS FOR REMOTE SENSING OF DENSITY.	5. TYPE OF REPORT & PERIOD COVERED: Scientific. ~~Intermin.~~
	6. PERFORMING ORG. REPORT NUMBER
7. AUTHOR(s): Roger A. Van Tassel	8. CONTRACT OR GRANT NUMBER(s): Technical rept.
9. PERFORMING ORGANIZATION NAME AND ADDRESS: Air Force Geophysics Laboratory (LKO), Hanscom Air Force Base, Massachusetts 01731	10. PROGRAM ELEMENT, PROJECT, TASK AREA & WORK UNIT NUMBERS: 62101F, 668806 ~~DMSP0011~~
11. CONTROLLING OFFICE NAME AND ADDRESS: Air Force Geophysics Laboratory (LKO), Hanscom Air Force Base, Massachusetts 01731	12. ~~REPORT DATE~~: 5 May 1978
	13. NUMBER OF PAGES: 20
14. MONITORING AGENCY NAME & ~~ADDRESS(if different from Controlling Office)~~: 29p.	15. SECURITY CLASS. *(of this report)*: Unclassified
	15a. DECLASSIFICATION/DOWNGRADING SCHEDULE

16. DISTRIBUTION STATEMENT *(of this Report)*

Approved for public release; distribution unlimited.

17. DISTRIBUTION STATEMENT *(of the abstract entered in Block 20, if different from Report)*

18. SUPPLEMENTARY NOTES

19. KEY WORDS *(Continue on reverse side if necessary and identify by block number)*

Airglow
Aeronomy
Remote sensing
Atmospheric density

20. ABSTRACT *(Continue on reverse side if necessary and identify by block number)*

An instrument to remotely determine neutral density profiles in the lower thermosphere has been developed by the Aerospace Corporation for use on the Defense Meteorological Satellite Program. The instrument observes ultraviolet airglow profiles in two bands: the 3371 Å band for nitrogen and the 1356 Å band for atomic oxygen to infer atmospheric density. Calculations of the intensities of these emissions have been made ~~at AFGL~~ by using the recent computations of energy-dependent photoelectron fluxes ~~by Jasperse~~ and experimental determinations of the excitation cross section. The results of these calculations are compared with profiles produced by a general representation developed by Stewart.

DD FORM 1 JAN 73 1473 EDITION OF 1 NOV 65 IS OBSOLETE

Unclassified

SECURITY CLASSIFICATION OF THIS PAGE *(When Data Entered)*

Preface

I wish to thank L. Heroux, J.R. Jasperse and C.M. Rush who generously provided their data as well as valuable suggestions and assistance. I also thank Marcel Schneeberger who did all of the computer programming for this project.

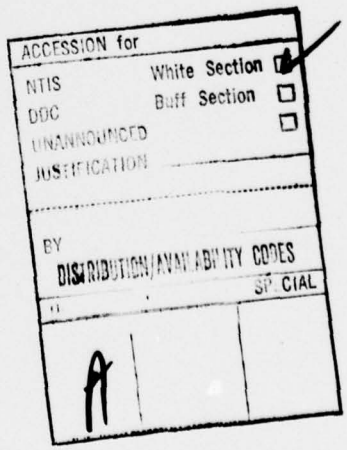

Contents

1. INTRODUCTION 7

2. CALCULATION OF VOLUME EMISSION RATES 8

3. LIMB VIEW COLUMN EMISSION 15

4. DISCUSSION 18

REFERENCES 20

Illustrations

1. Normalized Electron Distribution Function vs Energy for 130, 170 and 210 km 9

2. Apparent Cross Section for Electron-impact Excitation of the O-O Band of the Second Positive System of N_2 10

3. Cross Section for Electron-impact Excitation of the $^5S^\circ$ State in Atomic Oxygen 11

4. Emission Rates for the O-O Band of the Second Positive System at 3371 Å 12

Illustrations continued

5. Emission Rates from the $^5S^\circ$ State of O at 1356 Å 13

6. Calculated and Observed Electron Density Profiles 14

7. *Limb-viewing Geometry* 15

8. Column Emission Rates for the O-O Band of the Second Positive System of N_2 as Observed at the Satellite 16

9. Apparent Column Emission Rates from the $^5S^\circ$ State of Oxygen at 1356 Å as Observed at the Satellite 18

Tables

1. Fit Parameters for Excitation Efficiencies 14

Airglow Calculations for Remote Sensing of Density

1. INTRODUCTION

Unlike the near constancy of atmospheric density near the surface of the earth, atmospheric density in the thermosphere is highly variable. To forecast this density accurately, frequent realtime observations are necessary, just as accurate weather forcasts require observations of world-wide weather conditions. Forecasts of thermospheric density are required by the Air Weather Service. They are needed by those responsible for the tracking and control of low-altitude, earth orbiting satellites.

Presently these predictions are made from atmospheric models that describe the response of the atmosphere to phenomena such as changes in the solar ultraviolet flux and geomagnetic activity. While these models describe the behavior of the atmosphere reasonably well under quiet conditions, they cannot describe the behavior for short term departures from the average with the accuracy required for satellite ephemeris prediction.

To improve this situation, SAMSO is planning to fly a special ionospheric density sensor on the weather satellites which are part of the Defense Meteorological Satellite Program (DMSP). This sensor, designated the SSD, is being developed by the Aerospace Corporation[1] in an attempt to develop the capability to determine vertical density profiles remotely. This will overcome the limitation of conventional density measuring systems that can measure the density of the atmosphere only in a region through which the sensors pass.

(Received for publication 5 May 1978)

1. Hickman, D.R. (1977) The Remote Density Sensor, Aerospace Report No. TOR-0077 (263)-1, Aerospace Corporation, El Segundo, CA 90245.

The determination of vertical density profiles traditionally has been done with rockets because, unlike satellites, their trajectory is vertical through the atmosphere. A satellite system, however, has the advantage of collecting synoptic data for long periods of time.

To sound density remotely, the SSD makes use of the relationship between atmospheric density and the rate of production of certain optical emissions. The instrument itself is an ultraviolet spectrometer which scans the atmosphere above the earth at altitudes from 80 to 250 km. Two ultraviolet airglow emissions are used: the 3371 Å nitrogen band and the 1356 Å atomic oxygen doublet. Both are excited during the day by photoelectrons, which are themselves produced by photoionization of the ambient atmosphere by the extreme ultraviolet (EUV) radiation from the sun. The emission thus produced radiates in all directions and may be observed by the spectrometer on the satellite.

The problem of calculating the radiant intensity at the satellite from the volume emission rate in the atmosphere is relatively straightforward for these emissions because scattering may be neglected. The only radiative transfer complication which is significant is absorption of the 1356 Å emission by O_2 along the ray path.

The following procedure has been developed by Aerospace to infer atmospheric density from the airglow intensities:

1) a reasonable density profile is chosen using the present forecast methods,

2) airglow profiles for both the 3371 Å and the 1356 Å emissions are calculated using the assumed density profile,

3) The difference between the calculated airglow profiles and the observed airglow profiles is used to modify the density profiles.

These steps are repeated until there is substantial agreement between the calculated and observed airglow profiles. At this point the density profile is assumed to be correct.

In this report we give the results of detailed computations of airglow radiant intensity. The results are compared with profiles which are predicted using the more general representation presently planned for use by the Air Weather Service.

2. CALCULATION OF VOLUME EMISSION RATES

The rates for excitation to the upper states of the emitting species were calculated by evaluating the expression

$$q_{ex}(z) = 5.93 \times 10^{7}\, n(z) \int dE\; Q(E)\; 4\pi F\,(z,E)\; \sqrt{E}. \qquad (1)$$

Here $q_{ex}(z)$ is the excitation rate at altitude z; n(z) is the number density of nitrogen or atomic oxygen as appropriate; Q(E) is the excitation cross section; E is the electron energy in eV, and F(z,E) is the electron flux in $cm^{-2}\, sr^{-1}\, sec^{-1}\, eV^{-1}$.

Calculated values for the electron flux as a function of energy at several altitudes were provided

by Jasperse[2]. Jasperse computed these fluxes from coupled non-linear equations, derived using the Boltzmann-Planck method and the local approximation. He also calculated the fluxes by using the much simpler continuous slowing-down approximation. All the computations were made for the conditions that existed during the recent experiment where the solar spectral flux was measured by a rocket-borne spectrometer simultaneously with the electron concentration by a ground based ionosonde[3]. The solar spectral flux at the top of the ionosphere was that given by Heroux, the 10.7 cm solar flux was 120 x 10^{-22} W m^{-2} Hz^{-1}, the solar zenith angle was 27°, the local time was 1304, and the Jacchia[4] neutral particle exospheric temperature was 992°K. All other model ionospheric parameters are given in Jasperse. The fluxes for the energy range important for airglow production are shown for three altitudes in Figure 1.

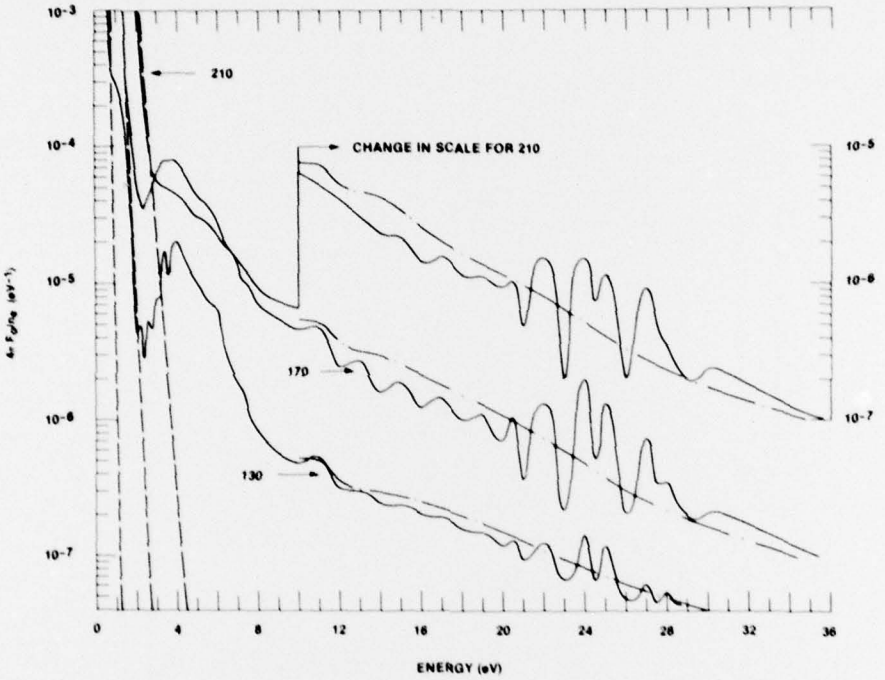

Figure 1. Normalized Electron Distribution Function vs Energy for 130, 170, and 210 km. Solid curves are calculated functions, dashed curves are curve-fitted normalized Maxwellian functions, and dot-dashed curves are normalized continuous slowing-down approximations. Solar zenith angle was 27°. (Reference 2)

2. Jasperse, J.R. (1977) Electron distribution functions and ion concentrations in the earth's lower ionosphere from Boltzmann-Fokker-Planck theory, Planet. Space Sci., 25, 743.
3. Heroux, L., Cohen, M., and Higgins, J.E. (1974) Electron densities between 110 and 300 km derived from EUV fluxes of August 23, 1972, J. Geophys. Res. 79, 5237.
4. Jacchia, L.G. (1971) Revised Static Models of the Thermosphere and Exosphere With Empirical Temperature Profiles, Spec. Report, 332, Smithsonian Astrophys. Observ., Cambridge, MA.

The detailed calculations show sharp structure in the electron spectra from 20 to 30 eV due to the photoionization of O and N_2 by the solar EUV HeII line at 40.8 eV. These features have been observed experimentally from a satellite by Doering, et. al.[5] and from a rocket by McMahon and Heroux[6]. The use of the continuous slowing-down approximation gives the average shape of the flux but does not give the detailed structure. The apparent cross section, Q(E), for electron impact excitation of the O-O band of the N_2 second positive system was taken from the experimental work of Jobe, et. al.[7] and is shown in Figure 2. The cross section is sharply peaked at 15 eV. The use of the

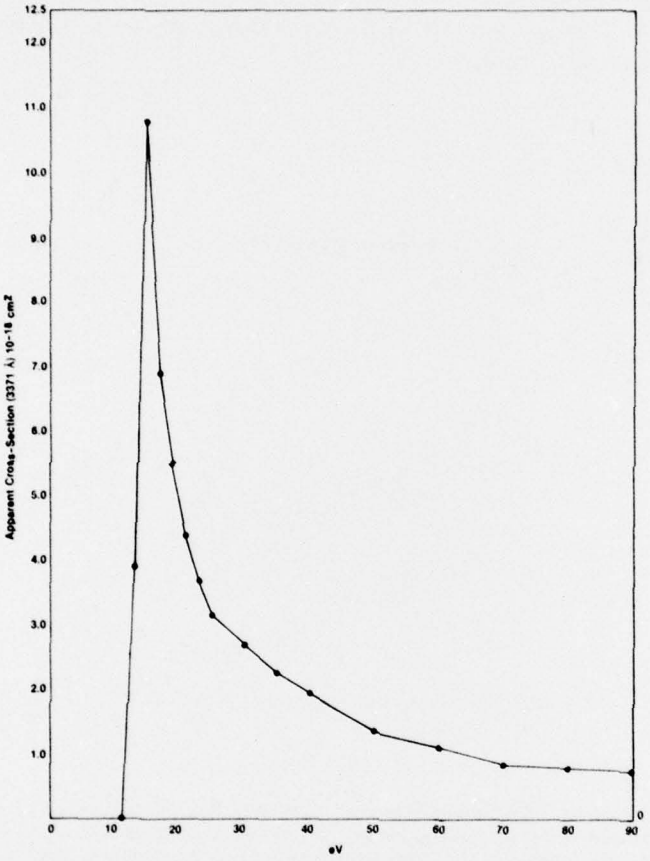

Figure 2. Apparent Cross Section for Electron-impact Excitation of the O-O Band of the Second Positive System of N_2 (Reference 7)

5. Doering, J.P., Peterson, W.K., Bostrom, C.O., and Armstrong, J.C. (1975) Measurement of low-energy electrons in the day airglow and day side auroral zone from Atmospheric Explorer C, J. Geophys. Res. 80, 3934.

6. McMahon, W.J., and Heroux, L. (January 13, 1977) Rocket Measurement of the Energy Distribution and Flux of Thermospheric Photoelectrons, AFGL-TR-77-0013, Air Force Geophysics Laboratory, Hanscom AFB, MA 01731.

7. Jobe, J.D., Sharpton, F.A., and St. John, R.M. (1967) Apparent cross sections of N_2 for electron excitation of the second positive system, J. Opt. Soc. Am., 57, 106.

apparent cross section to the upper state of the O-O band allows us to ignore cascading. The cross section for the excitation of the atomic oxygen doublet at 1356 Å was taken from the experimental work of Stone and Zipf[8] and is shown in Figure 3. Deactivation of the $^5S^\circ$ state by processes other than the emission of 1356 Å photons is unlikely, so the emission rate will effectively be equal to the excitation rate.

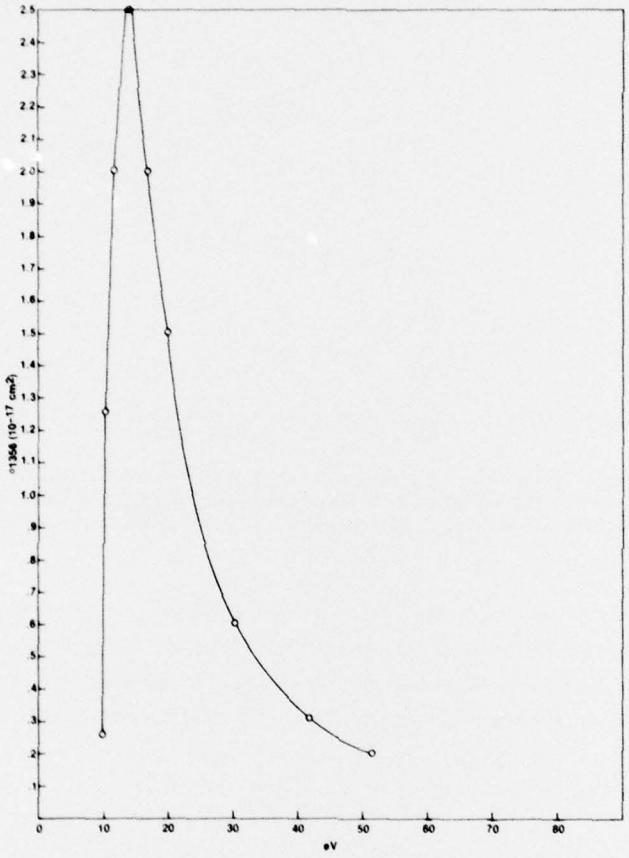

Figure 3. Cross section for Electron-impact Excitation of the $^5S^\circ$ State in Atomic Oxygen. (Reference 8)

Because the emission rates J(z) equal the excitation rates $q_{ex}(z)$ for both of these transitions, the solution of Eq. (1) gives the emission rates directly. This equation was solved at 16 altitudes between 97.5 km and 350 km using both the exact calculation of electron fluxes and the continuous slowing-down approximations. The results are shown in Figures 4 and 5. Interpolation between points was

8. Stone, E.J., and Zipf, E.C. (1974) Electron-impact excitation of the $^3S^\circ$ and $^5S^\circ$ states of atomic oxygen, J. Chem. Phys. 60, 4237.

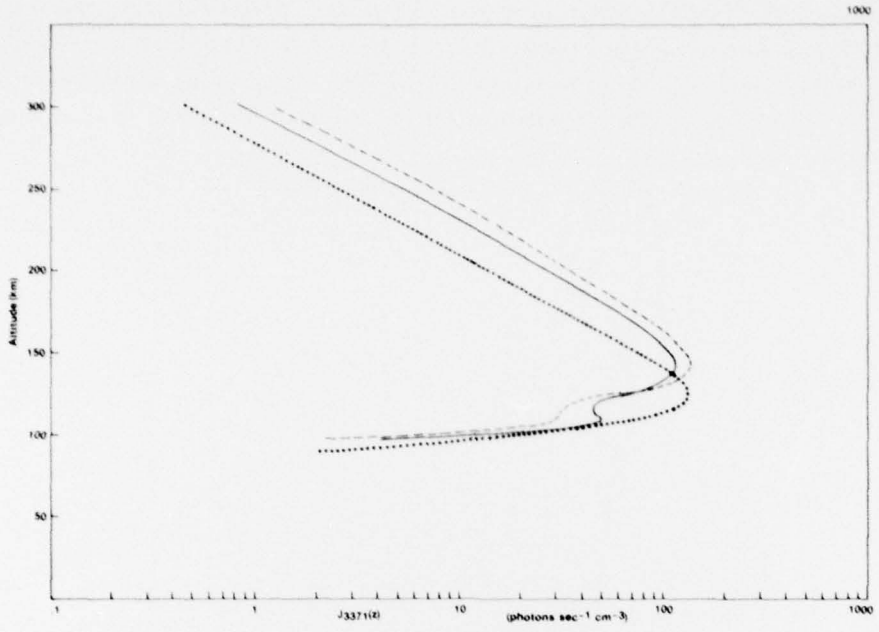

Figure 4. Emission Rates for the O-O Band of the Second Positive System at 3371 Å.
The solid curve uses electron fluxes using the detailed calculation of Jasperse; the dot-dash curve uses the results of the continuous slowing-down approximation, and the dotted curve uses the procedures developed by Stewart.

computed using a natural cubic spline function[9]. These emission rates are compared with calculations using procedures developed by Stewart[10] and programmed for use by Global Weather Central (GWC). Stewart used the calculations of Dalgarno et. al.[11] to represent the photoelectron excitation efficiencies as simple functions of an effective total slant-column density. A small correction being made for the local electron to neutral density ratio.

Using this procedure, the volume emission rate is given simply by

$$J_{ij}(z) = g_{ij}(z)\ \gamma_i\ n_i(z), \tag{2}$$

where $g_{ij}(z)$ is photoelectron impact excitation efficiency; γ_i is the branching ratio, and $n_i(z)$ is again the appropriate local number density. The n_i's used in this calculation are from the same Jacchia model as those used earlier. A value of 0.2 was used for γ_{3371} and 1.0 for γ_{1356}.

9. Greville, T.N.E. (1967) Spline functions, interpolation, and numerical quadrature, in Mathematical Methods for Digital Computers, Wiley.
10. Stewart, A.I. (1970) Photoionization coefficients and photoelectron impact excitation efficiencies in the daytime ionosphere, J. Geophys. Res. 75, 6333.
11. Dalgarno, A., McElroy, M.B., and Stewart, A.I. (1960) Electron impact excitation of the dayglow, J. Atmos. Sci., 26, 753.

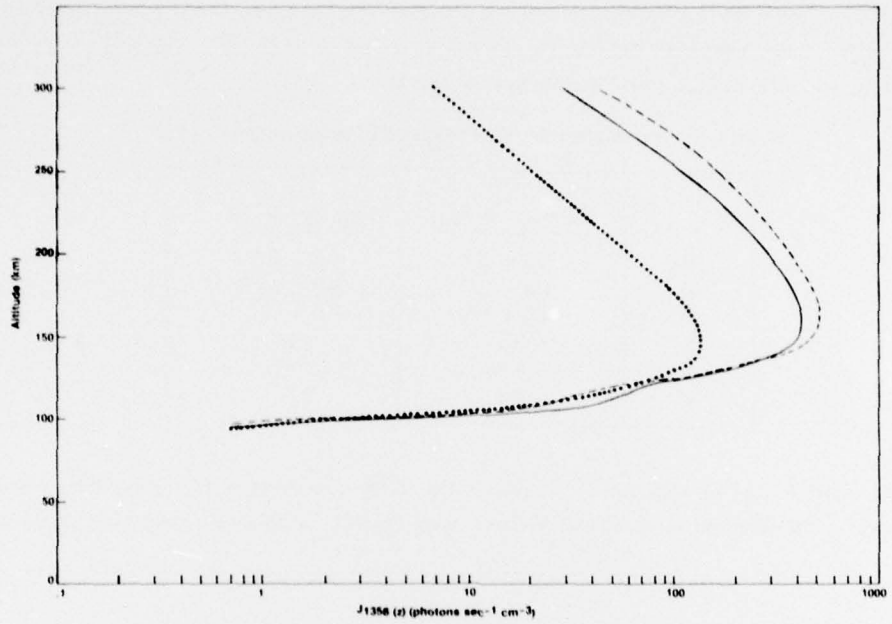

Figure 5. Emission Rates From the $^5S^\circ$ State of O at 1356 Å.
The solid curve uses electron fluxes using the detailed calculation of Jasperse; the dot-dash curve uses the results of the continuous slowing-down approximation, and the dotted curve uses the procedures developed by Stewart.

In the region where the effects of thermal electrons can be neglected, $g_{ij}(z)$ is given by

$$g_{ij}(z)^{-1} = B_o + B_1 (\tilde{N}(z)/10^{17}) + B_2(\tilde{N}(z)/10^{17})^{\beta}, \quad (3)$$

where the B's and β are given for the particular transition of interest. $\tilde{N}(z)$ is the effective total slant-column density of the neutral gases in the solar direction as given by

$$\tilde{N}(z) = 0.8\ N_O(z) + N_{O_2}(z) + N_{N_2}(z), \quad (4)$$

where the N_i's are the column density in the solar direction. At higher altitudes where the effects of thermal electrons can no longer be neglected, Stewart gives a correction to $g_{ij}(z)$ as

$$g_{ij}(z) = g_{ij}(\tilde{N}(z),\ r(z)) \simeq f_{ij}(r(z))\ g_{ij}(\tilde{N}(z),0). \quad (5)$$

Here r(z) is the electron/neutral ratio given by

$$r(z) = n_e(z) \ / \ \Sigma\ n_k(z). \quad (6)$$

The correction factor f(r) is given by $f = \exp\{-C(1 \times 10^2\, r(z))^\gamma\}$. Again, C and γ are selected for the particular states. Values for the B's, β's, C's and γ's are shown in Table 1. The N_i's were computed using the same Jacchia model atmosphere as used above.

Table 1. Fit Parameters for Excitation Efficiencies (Stewart, 1970)

	N_2 $C\ ^2\pi_u - B\ ^2\pi_g$	O $2p\ ^3S - 3s\ ^5S$
B_0	2.8×10^7	7.0×10^7
B_1	2.3×10^7	2.9×10^7
B_2	4.8×10^6	3.2×10^7
β	2.3	2.1
C	0.70	1.30
γ	0.9	0.7

The values for the electron density as used in Eq. (6) were determined by a three-dimensional ionospheric model described by Rush and Miller[12] using the ITS coefficients developed by Jones et

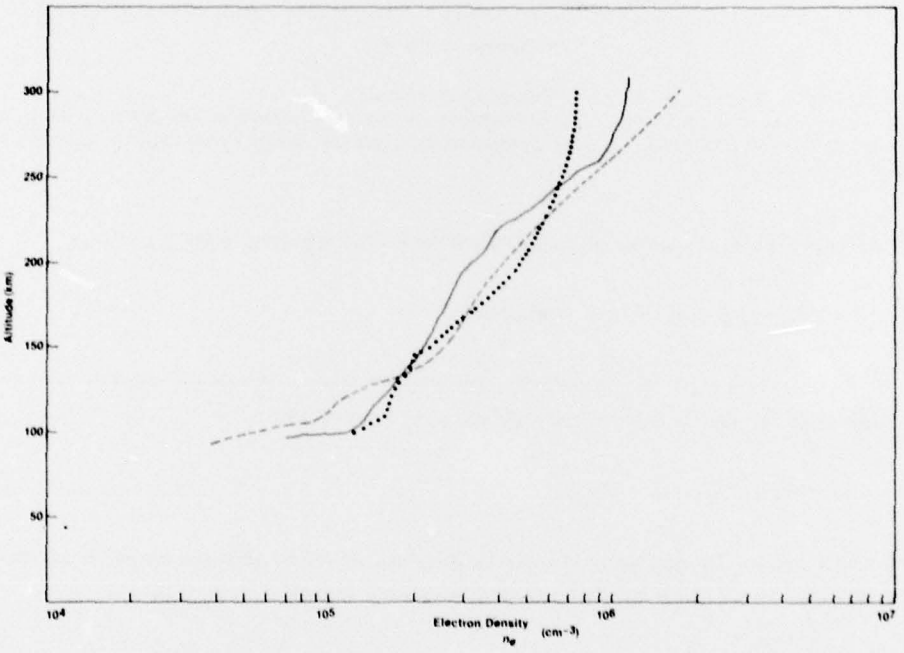

Figure 6. Calculated and Observed Electron Density Profiles. The dotted line is the profile calculated using the Rush-Miller model; the dashed line that given by Jasperse; and the solid line that measured by an ionosonde.

12. Rush, C.M., and Miller, D. (1973) A Three-Dimensional Ionospheric Model Using Observed Ionospheric Parameters, AFCRL-TR-73-0567. Air Force Cambridge Research Laboratories, Hanscom AFB, MA 01731.

al.[13]. The electron density profile obtained by this model is shown in Figure 6. It is compared with the profile which was calculated by Jasperse as well as with the profile which was measured by an ionosonde at the White Sands Missile Range at the time of the rocket flight.

3. LIMB VIEW COLUMN EMISSION

The intensity as observed at the satellite is calculated by integrating along the ray path defined by its grazing tangent height, h. The geometry is shown in Figure. 7.

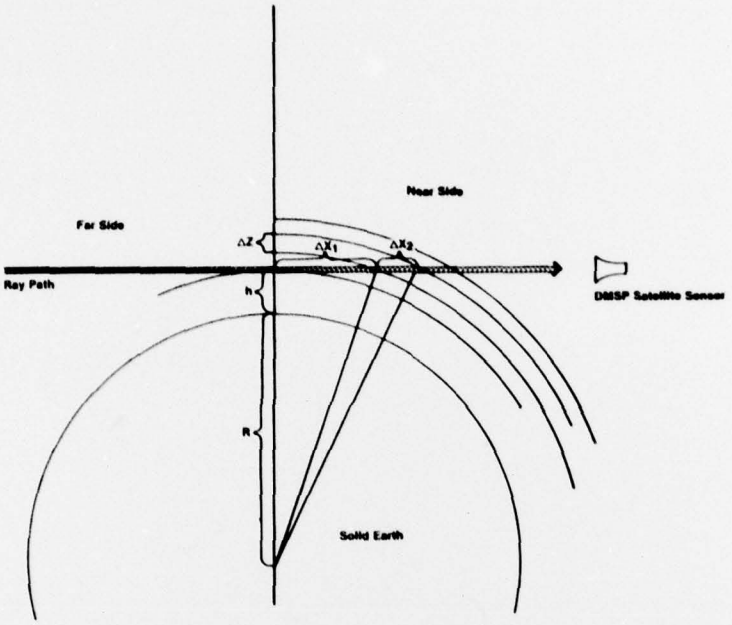

Figure 7. Limb-viewing Geometry

To perform the integration, the atmosphere is divided into spherical shells of thickness Δz km where z is the altitude. This divides the ray path into intervals of Δx km given by

$$\Delta x_n = \sqrt{(R_e + h + n\Delta z)^2 - (R_e + h)^2} - \Sigma \Delta x_{n-1}, \tag{7}$$

where R_e is the earth's radius, taken to be 6400 km; $\Delta x_0 = 0$.

The contribution of the emission in each increment is taken to be the average value of the volume emission within the increment multiplied by its length, Δx. Considering the double pass

13. Jones, W.B., Graham, R.P., and Leftin, M. and M. (1969) Advances in Ionospheric Mapping by Numerical Methods, ESSA Technical Report ERL 107-ITS 75, Institute for Telecommunication Sciences, Boulder, CO.

through the atmosphere, but neglecting absorption along the ray path gives

$$R(h) = 0.2 \sum_{n=1}^{\frac{800-h}{\Delta z}} \frac{J(h+n-1) + J(h+n)}{2} \Delta x(h)_n, \qquad (8)$$

where R(h) is the column emission in rayleighs (1 R is an apparent emission rate of 1 x 10^6 photons cm^2 (column) sec^{-1})[14]. The column emission from nitrogen at 3371 Å as calculated using Eq. 8 is shown in Figure 8.

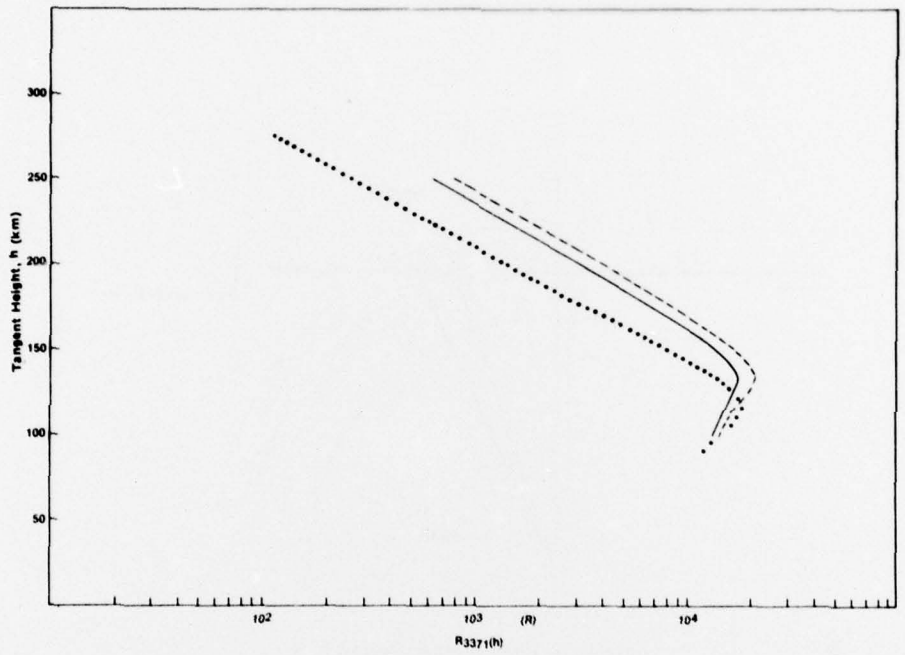

Figure 8. Column Emission Rates for the O-O Band of the Second Positive System of N_2 as Observed at the satellite. The solid curve uses electron fluxes using the detailed calculation of Jasperse; the dot-dash curve uses the results of the continuous slowing-down approximation, and the dotted curve uses the procedures developed by Stewart.

At 1356 Å, the absorption by molecular oxygen will be significant at the lower altitudes. To determine the column emission including the effects of absorption, the ray path was divided into two parts: the near side and the far side; the near side is between the satellite and the tangent point and

14. Chamberlain, J.W. (1961) Physics of the Aurora and Airglow, Academic Press, New York.

the far side is on the far side of the tangent point. The near side column emission is given by

$$R_{ns}(h) = 0.1 \sum_{n=1}^{\frac{800-h}{\Delta z}} \frac{J(h+n-1) + J(h+n)}{2} \Delta x(h)_n \exp -\sigma N(h)_n. \quad (9)$$

Here σ is the absorption cross-section for oxygen at 1356 Å, and N(h) is the total number of oxygen molecules between the emitting region and the satellite. The value of σ is taken as 8.5×10^{-18} cm^2 as given by Blake, et. al.[15].

The number of molecules between the emitting region and the satellite is given by

$$N(h)_n = 10^5 \left[\frac{n(h+n-1) + n(h+n)}{2} \frac{\Delta x(h)_n}{2} + \sum_{m=n+1}^{800-h} \frac{n(h+m-1) + n(h+m)}{2} \Delta x(h)_m \right]. \quad (10)$$

The first term represents molecules within the emitting region; the second term, molecules between the emitting region and the satellite. Although n is used as both a running integer and as a symbol for the oxygen number density, its use should be clear from the context.

The contribution from the far side is also given by Eq. 9, but in this case N(h) is given by

$$N(h)_n = 10^5 \left[\frac{n(h+n-1) + n(h+n)}{2} \frac{\Delta x(h)_n}{2} + \sum_{m+1}^{m=n+1} \frac{n(h+m-1 + n(h+m)}{2} \Delta x(h)_m + \right.$$

$$\left. \sum_{j=1}^{800-h} \frac{n(h+j) + n(h+j+1)}{2} \Delta x(h)_j \right]. \quad (11)$$

The first term is the contribution of the molecules within the emitting region; the second term is the contribution of molecules between the emitting region and the tangent point, and the third term is the contribution of molecules between the tangent point and the satellite.

The total column emission is the sum of the near-side and far-side contributions. The total column emission from atomic oxygen at 1356 Å is shown in Figure 9. The effect of neglecting molecular oxygen absorption is shown for comparison.

15. Blake, A.J., Carver, J.H. and Haddad, G.N. (1966) Photo-absorption cross-sections of molecular oxygen between 1250 Å and 2350 Å, J. Quant. Spectrosc. Radiat. Transfer, 6, 451.

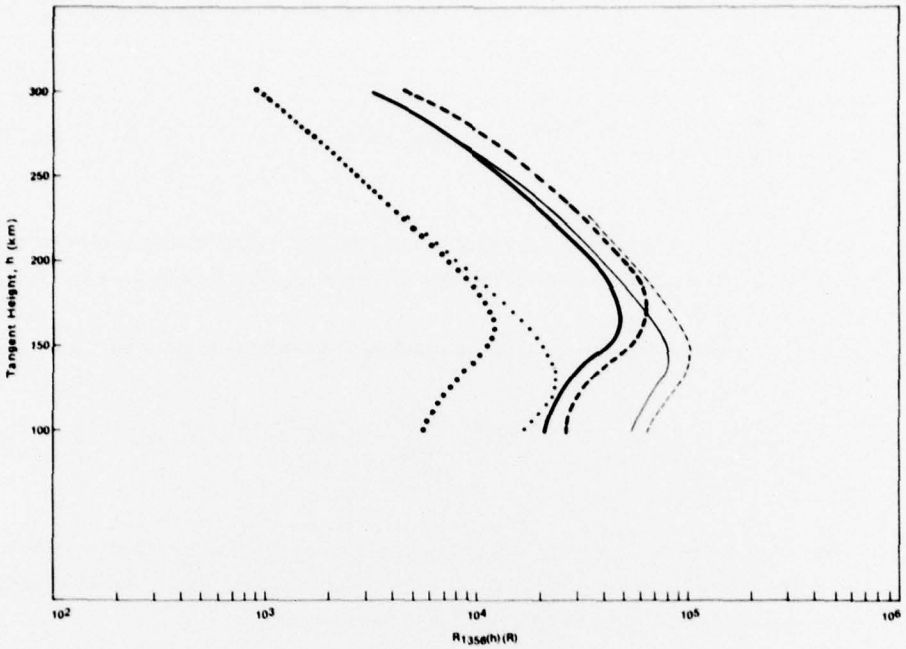

Figure 9. Apparent Column Emission Rates From the $^5S^\circ$ State of Oxygen at 1356 Å as Observed at the satellite. The solid curve uses electron fluxes using the detailed calculation of Jasperse; the dot-dash curve uses the results of the continuous slowing-down approximation, and the dotted curve uses the procedures developed by Stewart. The heavier lines include the effects of O_2 absorption.

4. DISCUSSION

Volume emission profiles for the 3371 Å nitrogen band and the 1356 Å atomic oxygen emission have been calculated using Jasperse computations of energy-dependent photoelectron fluxes and experimental determinations of the excitation cross sections. The results are compared with profiles produced by the general representation developed by Stewart. The same model for the neutral atmosphere has been used in all of the calculations.

Comparisons of the 3371 Å profiles show generally good agreement between the three curves (Figure 4), although the use of Jasperse flux data results in curves which gives the maximum in the emission about 20 km above that of Stewart. In addition, the use of the Jasperse flux results in a clearly defined E-region enhancement. The enhancement is less clearly defined when the continuous-slowing-down approximation is used. Even though the E-region enhancement is quite pronounced in the volume emission profile, it is barely observable in the corresponding limb view profile, indicating the degree of difficulty in inferring accurate volume emission profiles from limb view profiles, especially for altitudes below the altitude of maximum intensity.

Comparison of the 1356 Å profiles shows a large discrepancy due to the difference in the value which was used for the cross-section. The Stewart model was developed before an experimental determination of this cross-section was available. As a result, a cross-section with a magnitude and shape similar to the $1\ ^1s - 2\ ^3s$ transition in helium was used. It is recommended that the values of the volume emission rate which are evaluated on the basis of the Stewart model be increased by a factor of three to bring them into agreement with the detailed calculation made here. The difference in the altitude of the peak emission, similar to that found for the 3371 Å band, remains unexplained.

The effect of O_2 absorption on the 1356 Å column emission as viewed from the satellite is shown in Figure 9. The O_2 absorption becomes especially important below a tangent height of 175 km, with the reduction in intensity reaching a maximum near 130 km. The absorption of the 1356 Å emission by O_2 results in a coupling of the effect of the O and O_2 densities on the observed column emission. This makes it impossible to unambiguously infer both the O and O_2 densities from this emission profile alone.

An experiment to measure the solar EUV flux, the photoelectron flux, the 3371 Å airglow profile and total density profiles by means of two rockets flown simultaneously is being planned. These data will be compared with the results of calculations made for the conditions that exist during the time of the flight.

References

1. Hickman, D.R. (1977) The Remote Density Sensor, Aerospace Report No. TOR-0077 (263)-1, Aerospace Corporation, El Segundo, CA 90245.
2. Jasperse, J.R. (1977) Electron distribution functions and ion concentrations in the earth's lower ionosphere from Boltzmann-Fokker-Planck theory, Planet. Space Sci., 25, 743.
3. Heroux, L., Cohen, M., and Higgins, J.E. (1974) Electron densities between 110 and 300 km derived from EUV fluxes of August 23, 1972, J. Geophys. Res. 79, 5237.
4. Jacchia, L.G. (1971) Revised Static Models of the Thermosphere and Exosphere With Empirical Temperature Profiles, Spec. Report, 332, Smithsonian Astrophys. Observ., Cambridge, MA.
5. Doering, J.P., Peterson, W.K., Bostrom, C.O., and Armstrong, J.C. (1975) Measurement of low-energy electrons in the day airglow and day side auroral zone from Atmospheric Explorer C, J. Geophys. Res. 80, 3934.
6. McMahon, W.J., and Heroux, L. (January 13, 1977) Rocket Measurement of the Energy Distribution and Flux of Thermospheric Photoelectrons, AFGL-TR-77-0013, Air Force Geophysics Laboratory, Hanscom AFB, MA 01731.
7. Jobe, J.D., Sharpton, F.A., and St. John, R.M. (1967) Apparent cross sections of N_2 for electron excitation of the second positive system, J. Opt. Soc. Am., 57, 106.
8. Stone, E.J., and Zipf, E.C. (1974) Electron-impact excitation of the $^3S^\circ$ and $^5S^\circ$ states of atomic oxygen, J. Chem. Phys. 60, 4237.
9. Greville, T.N.E. (1967) Spline functions, interpolation, and numerical quadrature, in Mathematical Methods for Digital Computers, Wiley.
10. Stewart, A.I. (1970) Photoionization coefficients and photoelectron impact excitation efficiencies in the daytime ionosphere, J. Geophys. Res. 75, 6333.
11. Dalgarno, A., McElroy, M.B., and Stewart, A.I. (1960) Electron impact excitation of the dayglow, J. Atmos. Sci., 26, 753.
12. Rush, C.M., and Miller, D. (1973) A Three-Dimensional Ionospheric Model Using Observed Ionospheric Parameters, AFCRL-TR-73-0567, Air Force Cambridge Research Laboratories, Hanscom AFB, MA 01731.
13. Jones, W.B., Graham, R.P., and Leftin, M. and M. (1969) Advances in Ionospheric Mapping by Numerical Methods, ESSA Technical Report ERL 107-ITS 75, Institute for Telecommunication Sciences, Boulder, CO.
14. Chamberlain, J.W. (1961) Physics of the Aurora and Airglow, Academic Press, New York.
15. Blake, A.J., Carver, J.H. and Haddad, G.N. (1966) Photo-absorption cross-sections of molecular oxygen between 1250Å and 2350Å, J. Quant. Spectrosc. Radiat. Transfer, 6, 451.
16. Doering, J.P., Peterson, W.K., Bostrom, C.O., and Potemia, T.A. (1976) High resolution daytime photoelectron energy spectra from AE-E, Geophys. Res. Lett. 3, 129.
17. Garstang, R.H. (1961) Mutual magnetic interactions and oscillator strengths in the first spectrum of oxygen, Proc. Cambridge Phil. Soc., 57, 115-120.